6th European Conference on Computational Mechanics (ECCM 6)
7th European Conference on Computational Fluid Dynamics (ECFD 7)
11-15 June 2018, Glasgow, UK

COHESIVE ZONE MODELS OF SINGLE STEP JOINT DAMAGED DUE TO THE SHEAR CRACK

M. VERBIST[1], J.M. BRANCO[2] AND T. DESCAMPS[3]

[1] ISISE, University of Minho, DECivil
Campus de Azurém, 4800-058, Guimarães, Portugal
verbist.maxime@hotmail.com

[2] ISISE, University of Minho, DECivil
Campus de Azurém, 4800-058, Guimarães, Portugal
jbranco@civil.uminho.pt

[3] URBAINE, University of Mons, DSM,
Rue du Joncquois 53, 7000, Mons, Belgium
Thierry.DESCAMPS@umons.ac.be

Key words: Wood, Traditional Carpentry Connections, Design.

Summary. Being subject to the horizontal thrust from the carpentry, the Single Step Joint (SSJ) may be damaged due to the shear crack in the tie beam, entailing the collapse of the whole timber truss. In order to prevent this brittle failure mode, the reliability of SSJ design model against the shear crack must be improved by introducing the reducer coefficient $k_{v,red}$, taking into account the Hammock Shape Shear Stress Distribution (HSSSD), parallel to the grain at the heel depth in the tie beam. The HSSSD and reducer coefficient $k_{v,red}$ are significantly influenced by two SSJ geometrical parameters: i) the geometrical proportion between the shear length and heel depth l_v/t_v, and ii) the inclination angle α of the front-notch surface. The present study aims at determining the values of $k_{v,red}$ by comparing the numerical results through Finite Element Models (FEM) with the experimental results for several SSJ geometrical configurations tested. To this end, the HSSSD must be assessed through different parameters (e.g. average shear stress τ_m). In order to obtain a realistic curve of the HSSSD, a Cohesive Zone Model has been settled to simulate the shear crack parallel to the grain at the heel depth in the tie beam. The numerical results have shown a strong dependence between the average shear stress τ_m in the tie beam and both SSJ geometrical parameters α and l_v/t_v. Furthermore, the reducer coefficient $k_{v,red}$ has been determined as a product of two components: $k_{v,red,\alpha}$ and $k_{v,red,lv/tv}$. In addition of meeting both conditions $k_{v,red,\alpha} \geq 1$ and $k_{v,red,lv/tv} \leq 1$, empirical equations for both components of the reducer coefficient have been proposed in order to enhance the reliability of the SSJ design model against the shear crack.

1 INTRODUCTION

Being located at the foot of timber trusses, the Single Step Joint (SSJ) is subject to significant horizontal thrust from long-term and permanent axial compressive loads N_{rafter} in the rafter. Hence, this traditional carpentry connection may be damaged due to the shear crack at the heel depth t_v along the shear length l_v in the tie beam, as shown in Figure 1. This brittle failure mode has to be prevented since it entails the collapse of the whole timber truss. From a literature review, Verbist et al. [1] then proposed to check the SSJ design model (1) against the shear crack by introducing the reducer coefficient $k_{v,red}$ applied to the average shear strength of wood $f_{v,m}$. In fact, this coefficient takes into account the non-uniform shear stress distribution τ_{Ed} in the tie beam, also called Hammock Shape Shear Stress Distribution (HSSSD), resulting in reducing the shear capacity of the Single Step Joint. The other two SSJ geometrical parameters b and β stated in (1) are the width of the tie beam and the rafter skew angle, respectively.

$$N_{rafter} \leq k_{v,red} \cdot f_{v,m} \cdot \frac{b \cdot \min(l_v, 8.t_v)}{\cos\beta} \quad (1)$$

From previous numerical research conducted on some types of traditional carpentry joints linking the rafter to the tie beam [2-6], the HSSSD and reducer coefficient are significantly influenced by the geometrical parameters of the connection. As regards the SSJ, they depend on two geometrical parameters [5]: i) the geometrical proportion l_v/t_v between the shear length and heel depth, and ii) the inclination angle α of the front-notch surface.

In order to improve the reliability of the SSJ design model (1) against the shear crack, the present study aims at determining the values of $k_{v,red}$ based on numerical analysis, through simulating a realistic shear crack in the tie beam with the Cohesive Zone Models (CZM) for several SSJ geometrical configurations. As per both SSJ geometrical parameters α and l_v/t_v, the HSSSD must be assessed by determining some parameters (e.g. maximal shear stress τ_{max}, average shear stress τ_m along the shear length...). Based on these results, reliable empirical equations of the reducer coefficient $k_{v,red}$ have to be established.

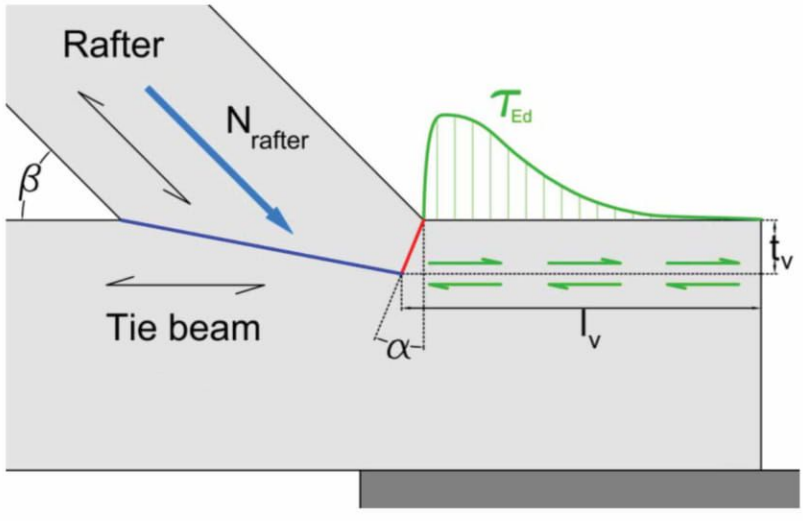

Figure 1: Non-uniform shear stress distribution τ_{Ed} and related shear crack at the heel depth t_v parallel to the grain along the shear length l_v in the tie beam.

2 NUMERICAL CAMPAIGN

The objective of the present study is to complete previous numerical researches [2-6] on the non-uniform shear stress distribution, by using the Cohesive Zone Models (CZM) to simulate the initiation and propagation of the shear crack in the Finite Element Models (FEM) of SSJ. To this end, the material, SSJ geometrical configurations of specimens tested, finite element modelling and research methodology have to be clearly defined.

2.1 Wood material

In Finite Element Models, wood can be considered as an orthotropic material, although it could also be featured by a transversal isotropy to simplify the material properties. Conform with the experimental data from Verbist et al. [1], it was decided to use *Pinus sylvestris* as wood species in the numerical work. Two different methods enable to obtain the material properties of wood species: either through carrying out several non-destructive and/or destructive tests for the wood mechanical characterization, or gathering information from a literature review.

Table 1 gives the material properties in average values for *Pinus sylvestris*. The compressive elastic moduli E_c along the grain (L) and perpendicular to the grain in respect with the radial (R) and tangential (T) directions were obtained from monotonic compression tests [1]. On the other hand, a literature review [7,8] was required in order to complete the lack of information for the other wood properties: Poisson's ratios ν, shear elastic moduli G, tensile strength $f_{t,90}$ perpendicular to the grain, shear strength f_v parallel and perpendicular to the grain, and last but not least the critical fracture energies G_C. Note that the parameters $f_{v,LR}$ from the Table 1 and $f_{v,m}$ from the equation (1) stand for the same wood mechanical property. For information, the average wood density of *Pinus sylvestris* is around 450 kg/m³ [1,8].

Table 1: Average values of wood properties for *Pinus sylvestris* [1,7,8].

Elastic moduli of compression and shear, and Poisson's ratios

$E_{c,L}$ [MPa]	$E_{c,T}$ [MPa]	$E_{c,R}$ [MPa]	ν_{LT}	ν_{LR}	ν_{TR}	G_{LT} [MPa]	G_{LR} [MPa]	G_{TR} [MPa]
7000	470	904	0.34	0.42	0.56	554	961	54

Tensile and shear strengths

$f_{t,90,T}$ [MPa]	$f_{t,90,R}$ [MPa]	$f_{v,LT}$ [MPa]	$f_{v,LR}$ [MPa]	$f_{v,TR}$ [MPa]
3.27	3.27	8	8	4

Fracture energies as per the three modes

$G_{C,I}$ [N/mm]	$G_{C,II}$ [N/mm]	$G_{C,III}$ [N/mm]
0.389	0.593	0.593

When modelling diverse possibilities of brittle failure mode inside wood, three types of displacements, also called cracking modes, are conceivable for the numerical analysis [4,7]. Being conditioned by the tensile strength $f_{t,90,R}$ and critical fracture energy $G_{C,I}$ perpendicular

to the grain, the mode I is related to the pure tensile cracking (i.e. opening deformation) perpendicular to the crack plane. On the other hand, the mode II and III deal with the crack propagation due to in-plane shear (i.e. slip deformation) and transverse shear respectively. The shear strength $f_{v,LR}$ and critical fracture energy $G_{C,II}$ parallel to the grain tie in with the mode II whereas the shear strength $f_{v,TR}$ and critical fracture energy $G_{C,III}$ perpendicular to the grain match the mode III. Since the present study aims at simulating the shear crack in the SSJ, input data from the mode II have to be settled carefully in the FEM.

2.2 Geometry of SSJ specimens

From the experimental work of Verbist et al. [1], nine SSJ geometrical configurations were picked up for modelling, since their respective normal load in the rafter N_{rafter} is governed by the shear crack in the tie beam. Those SSJ geometrical configurations are featured by the same rafter skew angle β=30° for which the positive contribution of friction forces at the front- and bottom-notch surfaces on the shear capacity is reduced. On the other hand, they differ from each other as per their inclination angle α of the front-notch surface and their geometrical proportion l_v/t_v between the shear length and heel depth. Indeed, both SSJ geometrical parameters significantly influence the non-uniform shear stress distribution in the tie beam, the shear capacity and then, the reducer coefficient $k_{v,red}$ [5]. Therefore, the inclination angle α has been varied between 0, 15 and 30 [°] whereas the geometrical proportion l_v/t_v has been taken as 160/30, 240/40, 240/30 and 240/25 [mm/mm].

In order to complete the present study on the non-uniform shear stress distribution in the tie beam, five geometrical proportions l_v/t_v were added for SSJ geometrical configurations featured by α=0°: 50/30, 75/30, 100/30, 125/30 and 200/30 [mm/mm]. In that way, it makes easier to establish the relationships of both SSJ geometrical parameters l_v/t_v and α, independently from each other, on the shear capacity of the tie beam and then, on both components of the reducer coefficient ($k_{v,red,lv/tv}$ and $k_{v,red,\alpha}$ respectively). In total, 14 SSJ geometrical configurations were modelled, by selecting the cross-section dimensions of timber joint elements: 100 x 100 mm for the rafter, and 100 x 160 mm for the tie beam. As a reminder, all the SSJ geometrical parameters quoted are illustrated in Figure 1.

2.3 Finite element modelling

In the numerical campaign, a 3D deformable solid was used to model in ABAQUS software all the SSJ geometrical configurations previously described, into three parts as illustrated in Figure 2: the rafter, the upper and bottom parts of the tie beam. For each part of the 3D model, an ideal linear elastic and orthotropic wood material was assumed as per the elastic compressive moduli E_c, Poisson's ratios ν and elastic shear moduli G for *Pinus sylvestris* given in Table 1.

The static analysis was selected to apply the monotonic compression loading at the top of the rafter parallel to the grain (N_{rafter}), conform with the experimental results of Verbist et al. [1] on SSJ specimens damaged due to shear crack. In order to get close to the realistic mechanical behaviour of the SSJ within the timber truss under permanent and long-term loads, two types of boundary conditions were implemented in the 3D model. As shown in Figure 2, the tie beam is simply supported with free end near the SSJ heel while the opposite

end at the back side of the connection is anchored, leading to stretching the tie beam parallel to the grain when loading the rafter in compression.

As regards the front-notch and bottom notch surfaces between the rafter and tie beam, two types of contact surface properties were settled: the tangential behaviour with isotropic coefficient of static friction μ_s=0.25 [9], and the normal behaviour featured by a "Hard" contact. On the other hand, the CZM was used at the interface between the upper and bottom parts of the tie beam, as a local approach to simulate the initiation and propagation of the shear crack at the heel depth over the shear length along the grain.

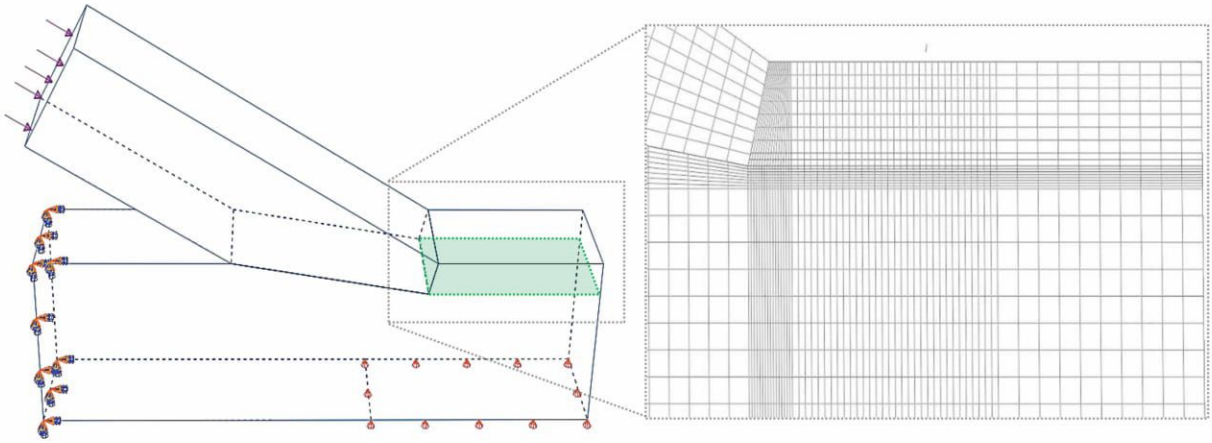

Figure 2: 3D model of Single Step Joint (left) and mesh strategy in the tie beam for the cohesive surface (right).

The CZM approach consists of modelling different brittle failure modes inside wood as per modes I, II or III previously described in the subsection "2.1 Wood material", based on damage mechanics (i.e. initiation, evolution and stabilization) and fracture mechanics. As a reminder, the scope of the study focuses on the simulation of the shear crack at the heel depth along the grain in the tie beam, conform with the mode II. To this end, a cohesive surface (i.e. zero-thickness element) was defined, at the interface between the upper and bottom parts of the tie beam, through different input properties for the linear traction separation-law already implemented in ABAQUS:

- Cohesive behaviour must be established through three stiffness parameters of the cohesive surface (K_I, K_{II}, K_{III}) in respect with modes I, II and III. In most of cases, stiffness parameters can be taken as 10^5N/mm³ in order to provide enough rigidity to the CZM requested for a good convergence of numerical results. However, this value was too high since unrealistic very pinched curve of the non-uniform shear stress distribution was recorded near the SSJ heel. Besides, the displacement of the upper part of the tie beam on the cohesive surface was too short, when comparing with the horizontal displacement from the experimental results [1]. Therefore, the stiffness parameters (K_I, K_{II}, K_{III}) were calibrated to the value 10^3 N/mm³;
- Damage initiation can be introduced with the data input of the tensile strength perpendicular to the grain ($f_{t,90,R}$), the shear strength parallel and perpendicular to the grain ($f_{v,LR}$ and $f_{v,TR}$), given in Table 1, as per modes I, II and III, respectively. Before initiating damage, the triangle traction-separation law implemented in ABAQUS was assumed as a linear elastic behaviour [4]. As soon as contact stresses satisfy for

example the maximum stress criterion (2) defined for the damage initiation, the stiffness of the cohesive surface starts to degrade. Note that the parameters $\sigma_{t,90,R}$, $\tau_{v,LR}$ and $\tau_{v,TR}$ stand for the tensile stress perpendicular to the grain, the shear strength parallel and perpendicular to the grain on the cohesive surface, respectively;

$$max\left\{\frac{\sigma_{t,90,R}}{f_{t,90,R}}\ ;\ \frac{\tau_{v,LR}}{f_{v,LR}}\ ;\ \frac{\tau_{v,TR}}{f_{v,TR}}\right\} = 1 \quad (2)$$

- Damage evolution depends on the definition of energy-based damage criterion through a function of mixed-mode fracture for which energies of each mode are dissipated as a result of the damage process. In fact, the fracture energy is equal to the area below the traction-separation law previously defined [4]. In the present study, Benzeggagh-Kenane (BK) function (3) implemented in ABAQUS was chosen to simulate the damage evolution, by taking into account the fracture energies released (G_I, G_{II} and G_{III}) and the critical fracture energies ($G_{C,I}$, $G_{C,II}$ and $G_{C,III}$) given in Table 1, as per modes I, II and III of wood cracking. Note that BK exponent η was taken as 2.284;

$$G_{C,I} + \left(G_{C,II} - G_{C,I}\right) \cdot \left(\frac{G_{II}+G_{III}}{G_I+G_{II}+G_{III}}\right)^{\eta} = G_{C,I} + G_{C,II} + G_{C,III} \quad (3)$$

- Damage stabilization should be specified in order to control the rate of convergence during the numerical calculations. To this end, the coefficient of viscosity for the cohesive surface was settled as 0.1.

As illustrated in Figure 2, a progressive mesh strategy was established in the vicinity of the cohesive surface at the heel depth of the tie beam along the shear length. Because accuracy of numerical results heavily depends on the elements size, it is recommended to refine the mesh as much as possible, although it will lead to increasing the calculation time. From previous numerical works [5], the maximal shear stress and the pinched curve of the non-uniform shear stress distribution were concentrated on a small area very close to the SSJ heel. Therefore, the mesh was refined over 80 mm length near the SSJ heel by assuming a thickness of elements equal to 1 mm. For information, each element from meshing the 3D model in ABAQUS was based on C3D8R which is an 8-node linear brick element with reduced integration.

2.4 Research methodology

Through modelling the shear crack in the SSJ, the research methodology firstly aims at defining better the non-uniform shear stress distribution τ_{Ed}, also called Hammock Shape Shear Stress Distribution (HSSSD) [5], at the heel depth t_v along the shear length l_v in the tie beam. To this end, several HSSSD parameters shown in Figure 3 can be introduced: the maximal shear stress τ_{max}, the average shear stress τ_m along the shear length, and last but not least, the shear concentration length l_{SC} along which the related average shear stress $\tau_{m,SC}$ has to be lower than the average shear strength of wood $f_{v,m}$ in order to prevent the emergence of shear crack in the tie beam. On the other hand, the shear concentration length vary as per the geometrical proportion l_v/t_v and cannot exceed the shear length l_v.The two average shear stresses (τ_m and $\tau_{m,SC}$) over the shear length and the shear concentration length can be calculated by equations (4) and (5) respectively.

$$\tau_m = \frac{\int_{l_v}^{0} \tau(x) \, . \, dx}{l_v} \tag{4}$$

$$\tau_{m,SC} = \frac{\int_{l_{SC}}^{0} \tau(x) \, . \, dx}{l_{SC}} \tag{5}$$

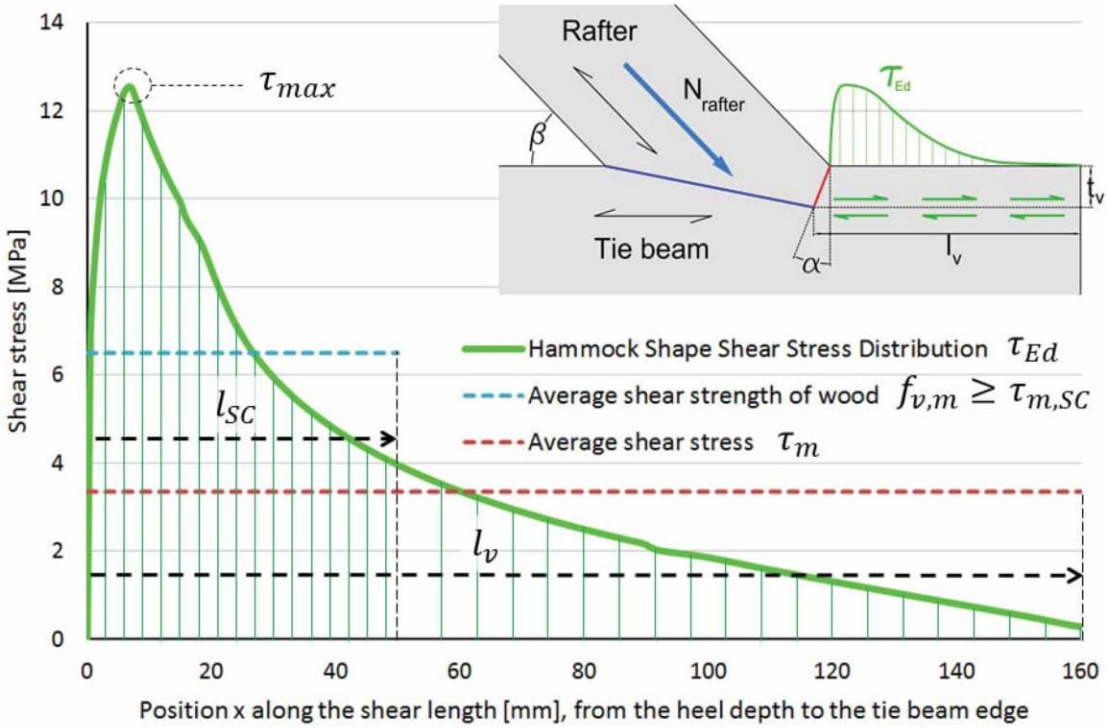

Figure 3: Parameters related to the Hammock Shape Shear Stress Distribution (HSSSD).

From the previous numerical works on the Notched Joints [4] and SSJ [5], it has been shown that the HSSSD significantly varies as per the geometry of the connection, such as two SSJ geometrical parameters α and l_v/t_v for instance. Besides, the HSSSD is featured by a non-uniform shear stress distribution at the heel depth along the shear length in the tie beam, resulting in reducing the shear capacity of the connection. Therefore, the reducer coefficient $k_{v,red}$ from the SSJ design model (1) is strongly related to the HSSSD parameters and it also depends on the inclination angle α of the front-notch surface and the geometrical proportion l_v/t_v between the shear length and heel depth.

Conform with Verbist et al. [5], both SSJ geometrical parameters, independently from each other, influence the reducer coefficient so that it can be expressed as a product of two factors (6): the component of the reducer coefficient $k_{v,red,lv/tv}$ related to the geometrical proportion l_v/t_v, and the component of the reducer coefficient $k_{v,red,\alpha}$ as per the parameter α. Based on the numerical results obtained for the HSSSD parameters τ_m and $\tau_{m,SC}$, equations (7) and (8) can be proposed in order to calculate both components of the reducer coefficient. Note that $\tau_{m,SC,\alpha}$ and $\tau_{m,SC,0}$ are the average shear stresses over the shear concentration length related to SSJ geometrical configurations characterized by inclination angles α and 0°, respectively, of

the front-notch surface. It becomes obvious than both equations (7)-(8) check the conditions $k_{v,red,lv/tv} \leq 1$ and $k_{v,red,\alpha} \geq 1$ [5]. Afterwards, empirical equations can be proposed to estimate the reducer coefficient $k_{v,red}$ in respect with both SSJ geometrical parameters α and l_v/t_v, with the aim of improving the reliability of design model (1) against the shear crack.

$$k_{v,red} = k_{v,red,lv/tv} \cdot k_{v,red,\alpha} \tag{6}$$

$$k_{v,red,lv/tv} = \frac{\tau_m}{\tau_{m,SC}} \tag{7}$$

$$k_{v,red,\alpha} = \frac{\tau_{m,SC,\alpha}}{\tau_{m,SC,0}} \tag{8}$$

3 RESULTS AND DISCUSSION

Numerical analysis was performed on several geometrical configurations of Single Step Joint (SSJ) through modelling the shear crack in the tie beam, by using the Cohesive Zone Model (CZM). From those FEM, the numerical results on the parameters of the Hammock Shape Shear Stress Distribution (HSSSD) and on both components of the reducer coefficient $k_{v,red}$ were then obtained and discussed below. Afterwards, empirical equations of the reducer coefficient were determined and applied in the SSJ design model (1) against the shear crack to check their reliability.

3.1 HSSSD parameters

As expected from the literature review [2-6], the non-uniform shear stress distribution shown in Figure 4 is confirmed at the heel depth t_v along the shear length l_v in the tie beam and on the modelled cohesive surface too. As illustrated in Figures 3 and 4, the HSSSD is featured by a peak of shear stress near the SSJ heel whereas the shear stress decreases along the shear length to the tie beam edge. It seems that modelling the shear crack through a cohesive surface softens the pinched curve of the HSSSD, becoming more realistic when compared with that from pure elastic 3D models featuring a higher rigidity in the tie beam [5]. Furthermore, a strongly pinched curve of HSSSD involves higher maximal shear stress τ_{max} very close to the SSJ heel, and lower average shear stress τ_m due to faster decrease of the shear stress along the grain to the tie beam edge. It should be noted that the stiffness parameters (K_I, K_{II}, K_{III}) highly condition the pinched feature of HSSSD. The higher the stiffness, the more the curve of HSSSD is pinched.

As detailed in Table 2, it can be shown for the SSJ geometrical configurations with $\alpha = 0°$ that the average shear stress τ_m along the shear length drops with the increase of the geometrical parameter l_v/t_v, whereas it reaches the maximal value, equal to the shear stress $\tau_{m,SC,0}$ along the concentration shear length l_{SC} (i.e. the average shear strength of wood $f_{v,m}$) for $l_v/t_v \leq 2.5$. Conversely, the average shear stress $\tau_{m,SC,0}$, which is estimated on the basis of empirical values of the geometrical proportion l_{SC}/t_v, does not significantly vary according to the parameter l_v/t_v, and can then be approximated as a mean value of 6.47 MPa.

When comparing the mean value of $\tau_{m,SC,0}$ with those of $\tau_{m,SC,15}$ and $\tau_{m,SC,30}$, it can be shown that the average shear stress $\tau_{m,SC,\alpha}$, which also stands for the shear strength of wood $f_{v,m,\alpha}$ under an inclined angle α to grain, raises with the increase of the inclination angle α of

the front-notch surface. The same observation can be made for the maximal shear stress τ_{max} and the average shear stress τ_m along the shear length. Furthermore, the maximal shear stress may slightly increase with the decrease of the geometrical proportion l_v/t_v. It should also be noted that the values recorded for the parameter $\tau_{m,SC}$ are lower than the shear strength $f_{v,LR}$=8 MPa implemented in the FEM, except from the SSJ specimens featured by α=30°.

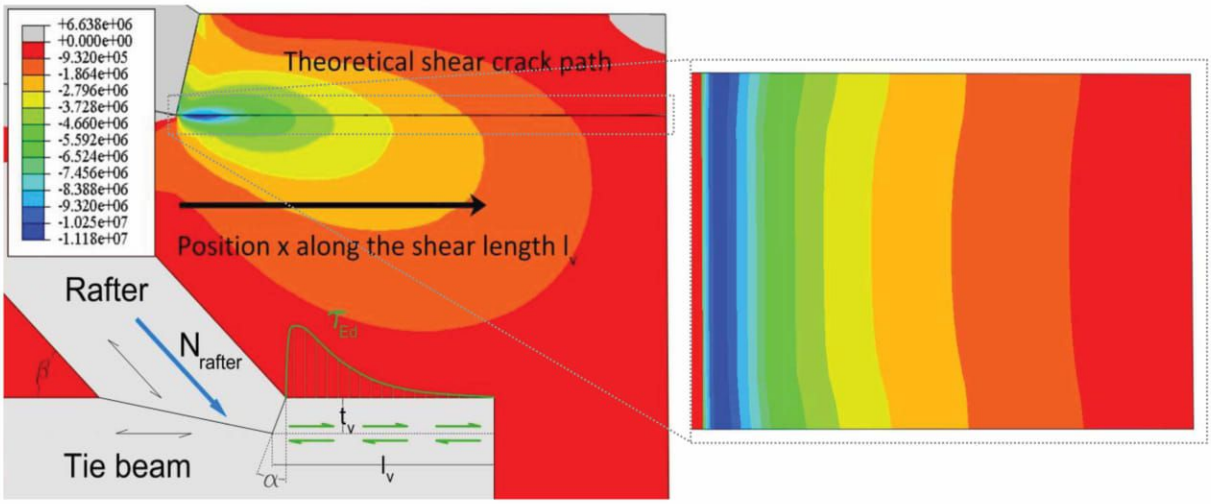

Figure 4: Non-uniform shear stress distribution τ_{Ed} [N/m²] parallel to the grain in the tie beam (left), and on the cohesive surface modelled at the heel depth t_v along the shear length l_v (right).

Table 2: Values of the HSSSD parameters obtained from the cohesive surface for different SSJ geometrical configurations investigated.

Specimens labelling	l_v/t_v	l_{SC}/t_v	N_{rafter} [kN]	τ_{max} [MPa]	$\tau_{m,SC}$ [MPa]	τ_m [MPa]
α0°_tv30_lv50	1.67	1.67	37	12.92	6.39	6.39
α0°_tv30_lv75	2.50	2.50	56	14.22	6.56	6.47
α0°_tv30_lv100	3.33	2.83	64	14.04	6.41	5.59
α0°_tv30_lv125	4.17	2.41	65	13.36	6.76	4.50
α0°_ tv30_lv160	5.33	1.83	60	12.32	6.67	3.21
α0°_ tv40_lv240	6.00	1.50	68	11.91	6.16	2.43
α0°_ tv30_lv200	6.67	1.62	61	11.89	6.76	2.59
α0°_ tv30_lv240	8.00	1.87	63	11.84	6.16	2.21
α0°_ tv25_lv240	9.60	2.17	62	11.92	6.36	2.15
α15°_ tv30_lv160	5.60	1.70	65	12.54	7.45	3.35
α15°_ tv40_lv240	6.27	1.55	70	11.99	6.30	2.43
α30°_ tv30_lv160	5.91	1.54	75	13.16	8.77	3.68
α30°_ tv40_lv240	6.58	1.61	97	13.64	8.22	3.21
α30°_ tv30_lv240	8.58	1.98	90	13.569	8.37	3.00

3.2 Reducer coefficient

From the assessment of the HSSSD parameters detailed in Table 2, other numerical results can be obtained for both components of the reducer coefficient ($k_{v,red,lv/tv}$ and $k_{v,red,\alpha}$), from the equations (7)-(8) previously defined. As illustrated in Figure 5, the component of the reducer coefficient $k_{v,red,lv/tv}$ starts dropping significantly ($k_{v,red,lv/tv} \ll 1$) as soon as the geometrical proportion l_v/t_v between the shear length and heel depth becomes higher than 2.5. On the other hand, the decrease of the coefficient slows down for $l_v/t_v \geq 6$, and a plateau seems to be reached with a minimal value of $k_{v,red,lv/tv}$=0.35 for high geometrical proportions ($l_v/t_v \geq 8$). This could be explained by the fact that the shear stress cannot be distributed in the tie beam over a shear length higher than 8 t_v, as expected from the design model against the shear crack [1]. On the other side of the graph, another plateau with a value of $k_{v,red,lv/tv}$=1 can be inferred for very low geometrical proportions ($l_v/t_v \leq 2.5$), by featuring no reduction of the shear strength $f_{v,m}$.

As shown in Figure 6, the component of the reducer coefficient goes up at a progressively increasing rate ($k_{v,red,\alpha} \geq 1$) as soon as the inclination angle α of front-notch surface becomes higher than 0°. Based on those observations and numerical results, empirical equations (9)-(10) and (11), with R^2= 0.998 and 0.96, respectively, were established and plotted in Figures 5 and 6, in order to estimate both components of the reducer coefficient ($k_{v,red,lv/tv}$ and $k_{v,red,\alpha}$), as per both SSJ geometrical parameters l_v/t_v and α.

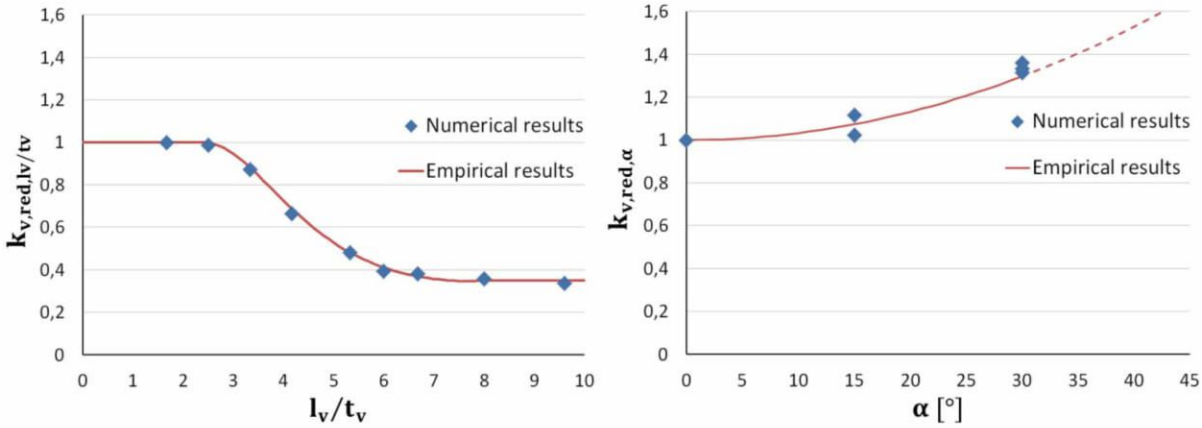

Figures 5 and 6: Evolution of both components of the reducer coefficient ($k_{v,red,lv/tv}$ and $k_{v,red,\alpha}$) as per the geometrical proportion l_v/t_v between the shear length and heel depth (left), and the inclination angle α of the front-notch surface (right).

$$k_{v,red,lv/tv} = \frac{k}{\frac{20}{7}.\sin^2\left(\frac{\pi}{11}.\left(\frac{l_v}{t_v}-3\right)\right)+cos^2\left(\frac{\pi}{11}.\left(\frac{l_v}{t_v}-3\right)\right)} \quad (9)$$

$$k = \frac{1}{-0.00716\,.\,\left(\frac{l_v}{t_v}\right)^2+0.07516\,.\left(\frac{l_v}{t_v}\right)+0.85684} \quad (10)$$

$$k_{v,red,\alpha} = \frac{1}{3000}.\alpha^2 + 1 \quad (11)$$

In order to check the efficiency of those empirical equations in term of enhancing the reliability of the SSJ design model against the shear crack (1), the experimental normal loads $N_{rafter,exp}$ in the rafter obtained from Verbist et al. [1] were compared with the updated theoretical ones $N_{rafter,theo}$, for each SSJ geometrical configuration damaged due to the shear crack. To this end, the relative variation $\Delta_{rel,rafter}$ [%] between the experimental and theoretical normal loads in the rafter was defined in (12). Conform with the numerical results of the average shear stress $\tau_{mSC;0}$ (Table 2), the average shear strength of wood $f_{v,m}$ was taken as 6.5 MPa for the theoretical calculations. As detailed in Table 3, the values of the reducer coefficient $k_{v,red}$ were determined based on the equations (6)-(9)-(10)-(11). It can be shown that the updated SSJ design model (1) against the shear crack with the empirical equations of the reducer coefficient is highly reliable ($\Delta_{rel,rafter}$<10%). However, it may be a little less reliable ($\Delta_{rel,rafter}$=11.4%) for the SSJ geometrical configuration featured by an inclination angle of the front-notch surface α=15° and by a geometrical proportion between the shear length and heel depth l_v/t_v=6.

$$\Delta_{\text{rel,rafter}}=100.\,(N_{rafter,exp}-N_{rafter,theo})/N_{rafter,theo} \tag{12}$$

Table 3: Comparison between the experimental and theoretical results for the SSJ geometrical configurations tested, by introducing values of the reducer coefficient $k_{v,red}$ from empirical equations (9)-(10)-(11).

Specimens labelling	$k_{v,red,lv/tv}$	$k_{v,red,\alpha}$	$k_{v,red}$	$N_{rafter,exp}$ [kN]	$N_{rafter,theo}$ [kN]	$\Delta_{\text{rel,rafter}}$ [%]
α0°_ tv30_lv160	0.48	1.00	0.48	60	57.64	4.09
α0°_ tv40_lv240	0.41	1.00	0.41	68	73.85	7.92
α0°_ tv30_lv240	0.35	1.00	0.35	63	63.05	0.08
α0°_ tv25_lv240	0.35	1.00	0.35	62	63.05	1.66
α15°_ tv30_lv160	0.45	1.07	0.48	65	60.54	7.37
α15°_ tv40_lv240	0.39	1.07	0.42	70	79.03	11.4
α30°_ tv30_lv160	0.42	1.30	0.55	75	73.2	2.46
α30°_ tv40_lv240	0.37	1.30	0.48	97	94.78	2.34
α30°_ tv30_lv240	0.36	1.30	0.47	90	90.77	0.85

4 CONCLUSION

In order to enhance the reliability of the design model of Single Step Joint (SSJ) against the shear crack, Finite Element Models (FEM) were performed for several SSJ geometrical configurations, by using a Cohesive Zone Model (CZM) for the simulation of the shear crack in the tie beam. From the numerical results obtained in the present study, it can be concluded:

- Parameters featuring the Hammock Shape Shear Stress Distribution in the tie beam were defined and assessed by modifying the inclination angle α and the geometrical proportion l_v/t_v between the shear length and heel depth;
- Reducer coefficient $k_{v,red}$ was inferred from both average shear stresses τ_m and $\tau_{m,SC}$, which highly depend on both SSJ geometrical parameters previously quoted;

- Reducer coefficient $k_{v,red}$ was expressed as a product of two independent components, in respect with the SSJ geometrical parameters α and l_v/t_v, by meeting beforehand both conditions $k_{v,red,\alpha} \geq 1$ and $k_{v,red,lv/tv} \leq 1$;
- Last but not least, efficient empirical equations of the reducer coefficient $k_{v,red}$ have been determined, resulting in improving strongly the reliability of the SSJ design model against the shear crack.

ACKNOWLEDGEMENTS

This work was financed by FEDER funds through the Competitively Factors Operational Programme – COMPETE and by national funds through FCT – Foundation for Science and Technology within the scope of the project "Invisible Woods" PTDC/EPH-PAT/2401/2014 and PhD Scholarships SFRH/BD/128580/2017.

REFERENCES

[1] Verbist, M., Branco, J.M., Poletti, E., Descamps, T., Lourenço, P. (2017). Single Step Joint: overview of European standardized approaches and experimentations. *Journal of Materials and Structures* – 50: 161 – March 27, 2017. DOI 10.1617/s11527-017-1028-4

[2] Villar, J.R., Guaita, M., Vidal, P., Arriaga, F. (2007). Analysis of the Stress State at the Cogging Joint in Timber Structures. *Biosystems Engineering* – Volume 96, Issue 1, pp 79-90 – January 2007.

[3] Faye, C., Garcia, P., Magorou, L.L., Rouger, F. (2008). Mechanical behaviour of traditional timber connections: proposals for design, based on experimental and numerical investigations. Part 1: birdsmouth. *CIB – W18. Meeting 41*, August 24-28, 2008, St. Andrews, Canada.

[4] Aira, J.R., Descamps, T., Van Parys, L., Léoskool, L. (2015). Study of stress distribution and stress concentration factor in notched wood pieces with cohesive surfaces. *European Journal of Wood and Wood Products* – Volume 73, Issue 3, pp 325-334 – May 2015.

[5] Verbist, M., Branco, J.M., Descamps, T. (2017). Hammock Shape Shear Stress Distribution in the Single Step Joint. *ECCOMAS Thematic Conference, CompWood 2017: Computational Methods in Wood Mechanics - from Material Properties to Timber Structures*. June 7-9, 2017, Vienna, Austria. (Seminar - Oral communication)

[6] Villar-García, J.R., Crespo, J., Moya, M., Guaita, M. (2018). Experimental and numerical studies of the stress state at the reverse step joint in heavy timber trusses. Materials and Structures – 51:17 – January 2018. DOI 10.1617/s11527-018-1144-9

[7] Danielsson, H. (2013). *Perpendicular to grain fracture analysis of wooden structural elements – Models and applications*. Doctoral Thesis, Structural Mechanics, Lund University. January 1, 2013, Lund, Sweden.

[8] Kretschmann, D.E. (2010). Chapter 5 – Mechanical Properties of Wood. *Wood Handbook – Wood as an Engineering Material*. Robert J. Ross (Eds.), USDA Forest Service, Forest Products Laboratory. April 2010, Madison (Wisconsin), USA.

[9] Aira, J.R., Arriaga, F., Íñiguez-González, G., Crespo, J. (2014). Static and kinetic friction coefficients of Scots pine (Pinus sylvestris L.), parallel and perpendicular to grain direction. *Materiales de Construcción*, Vol. 64, Issue 315. July-September 2014.